

Irreversible Injury of Isolated Adult Rat Myocytes

Osmotic Fragility During Metabolic Inhibition

CHARLES E. GANOTE, MD, and
RICHARD S. VANDER HEIDE, PhD

*From the Department of Pathology, Northwestern University
Medical School, Chicago, Illinois*

Isolated myocytes can be established as a valid model for studying changes in cytoskeletal proteins during the development of irreversible injury only if isolated cells develop lesions similar to those that occur during irreversible injury to intact hearts, specifically osmotic fragility and subsarcolemmal blebs. In the first experiment, isolated cells were irreversibly injured by metabolic inhibition with 5 mM Iodoacetic acid (IAA) and 6 mM amobarbital (Amy). Osmotic fragility of control and injured cells was determined by comparing the rates of development of trypan blue permeability during 60 minutes of isotonic or hypotonic (50% reduction in osmolality) incubations. Cell morphology was monitored by light and electron microscopy. Control cells remained elongated and excluded trypan blue. Metabolically inhibited cells rapidly contracted to a nearly square shape. The inhibited squared cells initially excluded trypan blue, but during 60 minutes of incubation became permeable to trypan blue. Cells in hypotonic buffer developed blue staining at a more rapid

rate than cells in isotonic buffer, indicating increased osmotic fragility. In a second experiment, control and inhibited cells were first incubated for 25 minutes in isotonic buffer and then in either isotonic or hypotonic buffer. In this experiment, inhibited cells also developed more extensive and rapid permeability increases when transferred to the hypotonic buffer than cells maintained in the isotonic buffer. In both experiments, increased permeability of cells to trypan blue was accompanied by formation of subsarcolemmal blebs along the lateral cell border and at the intercalated disks. The results show that metabolically inhibited, isolated myocytes do exhibit morphologic lesions and increased osmotic fragility properties similar to those reported during anoxic or ischemic injury to intact hearts. Therefore, isolated myocytes may be a useful model with which to study cytoskeletal-sarcolemmal membrane changes during development of irreversible injury. (*Am J Pathol* 1988, 132:212-222)

NORMAL HEART CELLS can be subjected to osmotic swelling by solutions with osmolalities as low as 60 mOsm without apparent injury.¹ In contrast, anoxic rat hearts and ischemic dog hearts are osmotically fragile. They suffer severe sarcolemmal damage when subjected to osmotic swelling, with release of cytosolic enzymes to the extracellular space and admittance of extracellular markers to the cytosolic space. The onset of osmotic fragility is closely associated with the onset of irreversible injury (susceptibility of the cells to the oxygen paradox and reperfusion damage).² In irreversibly injured ischemic and anoxic cells, the plasma membrane detaches from lateral Z-band costamere junctions, forming subsarcolemmal blebs. In the ischemic hearts, there is also a loss of immunofluorescence staining for the cytoskeletal protein vinculin.³ The authors have reported a loss of

staining for both alpha-actinin and vinculin in anoxic hearts.⁴ Vinculin forms part of a membrane-associated complex of proteins that binds actin to plasma membranes. Alpha-actinin crosslinks the branched ends of actin in Z-bands and at intercalated disks. The loss of cytoskeletal binding proteins (such as vinculin and alpha-actinin) could account for the formation of large subsarcolemmal blebs and for separations of terminal actin filaments from the internal face of intercalated disks that occur in swollen or mechanically damaged hearts. These lesions in turn could account for

Supported by American Heart Association Grant 86-674.
Accepted for publication March 11, 1988.

Address reprint requests to Charles E. Ganote, MD, Department of Pathology, Northwestern University Medical School, 303 East Chicago Avenue, Chicago, IL 60611.

the osmotic and mechanical fragility of irreversibly injured myocytes.

Biochemical study of the development of such lesions in intact tissues is complicated by the presence of vascular and other contaminating interstitial components. These tissue components have many of the same cytoskeletal proteins as the myocytes. The isolated adult myocyte would therefore seem to be a better model for the study of small changes in specific proteins of myocytes during injury. It has not, however, been established that anoxia or ischemia produces the same pattern of injury in isolated cells as occurs in intact tissues, because neither an oxygen nor a calcium paradox occurs in isolated myocytes.⁵⁻⁷ It has been hypothesized that the absence of these phenomena in isolated cells is not due to differences in basic mechanisms of injury, but rather is due to the absence of cell-to-cell contacts (and consequent mechanical injury) in freely floating isolated cells when they undergo hypercontracture during reoxygenation or readmission of calcium.⁵⁻¹⁰ Demonstration that osmotic fragility and morphologic lesions similar to those seen in intact tissues also occur in injured isolated myocytes, would provide evidence to support the hypothesis that injury occurring in isolated cells is indeed similar to that occurring in intact tissues.

In the present study isolated myocytes were subjected to metabolic inhibition to induce severe and rapid energy depletion. The rate of development of irreversible injury, as manifested by changes in osmotic fragility and cell morphology, during isotonic and hypotonic incubations was monitored. It was found that isolated myocytes do develop lesions similar to those described in intact tissues. These results suggest that isolated myocytes are a useful model with which to study cytoskeletal-sarcolemmal membrane changes during development of irreversible injury.

Materials and Methods

Cell Isolation

Isolated adult rat heart cells were prepared as described previously¹¹ using a modification of the technique of Altschuld et al.¹² Male Sprague-Dawley rats weighing 250–350 g were anesthetized by intraperitoneal injection of 55 mg/kg sodium pentobarbital (Diabul, Diamond Laboratories, Des Moines, IA). Following intravenous administration of 2000 IU sodium heparin (Elkins-Sinn), hearts were removed and immersed in ice cold perfusion solution. The solution was a nominally calcium-free ($\text{Ca}^{2+} < 25 \mu\text{M}$ by atomic adsorption spectrophotometry) buffer containing NaCl (90 mM), KCl (30 mM), NaHCO_3 (25

mM), KH_2PO_4 (1.2 mM), bovine serum albumin (BSA) (1 mg/ml) (Pentex Fraction V), MgCl_2 (1.2 mM), glucose (11 mM), taurine (60 mM), creatine (20 mM), and a complete amino acid solution. Final osmolarity measured with an Advanced Instruments freezing point osmometer was 360 mOsm. The heart was flushed with cold solution, then cannulated on a pump-driven Langendorff apparatus and perfused in a nonrecirculating mode for 5 minutes at 37 C. Collagenase (Class II, Cooper Biomedical, Malvern, PA) was then added (1.25 mg/ml) and the hearts were perfused in a recirculating mode until they became soft (45–60 minutes). During perfusion the buffer was gassed with 95% O_2 –5% CO_2 at pH 7.4. The hearts were then removed from the perfusion apparatus and minced in 5 ml perfusion buffer containing 4% wt/vol BSA. Following dispersion with a large bore pipet, the cells were transferred to a Nalgene flask and incubated in a shaking water bath at 30 C under air for 10 minutes. After filtering through a nylon mesh, the cells were washed in 5mM KCl (low K^+) buffer containing 5 mg/ml BSA, and again in low K^+ buffer containing 20 mg/ml BSA by 1 minute centrifugations at 75g in a tabletop centrifuge. The wash solutions contained, in addition to the buffer constituents, 10 mM HEPES as an additional buffer. Calcium was then added stepwise to a concentration of 1.12 mM. Viable cells, both calcium-tolerant and round, were differentially concentrated by virtue of their higher density than nonviable cells by low speed centrifugation (20g) for 1–2 minutes. The supernatant was discarded, and the cells washed twice more in 30 mM KCl buffer containing 1.12 mM calcium and 2% BSA using low speed centrifugations. The remaining cells were then resuspended in 10 ml of the final wash solution that was used for the subsequent incubations. Approximately 12 million cells were obtained from each isolate. Reagent grade iodoacetic acid was obtained from Sigma and amobarbital was obtained from Eli Lilly and Company (Indianapolis, IN).

Experimental Design

The first experiment investigated the effects of sustained isotonic or hypotonic incubations on cell viability and morphology. Cells were harvested as described above, but were divided into 2 groups for the final slow-speed spin. Each group of cells was then resuspended into 5 ml of either isotonic (360 mOsm) medium or 5 ml of hypotonic medium (2.5 ml buffer plus 2.5 ml deionized water). Each group of cells was then again subdivided into 2 incubation flasks (4 flasks total), each containing 2.5 ml of either isotonic

or hypotonic cells. To each flask was added either 2.5 ml of buffer of appropriate tonicity containing either 3 mM amobarbital (Amy) and 5 mM iodoacetic acid (IAA) or buffer without inhibitors. It was found in the course of the experiments that the amobarbital had become progressively less potent. This was reflected in a reduction in the rate and extent of cell squaring during incubations. The concentration of amobarbital was therefore increased in the final 5 experiments from 3 to 6 mM, so that 85–90% of cells again became square within 15 minutes of incubation. The dose of 5 mM IAA was chosen to ensure complete inhibition of glycolysis. Preliminary experiments using perfused rat hearts, had shown that doses of 1, 3, 5, and 10 mM IAA produced progressively more severe oxygen paradox injury when such doses were present during 45 minutes of anoxic perfusion followed by reoxygenation. The impression that high doses of IAA are needed to inhibit glycolysis in intact cells was confirmed by Dr. Ruth Altschuld, who found that 3–5 mM IAA is required to completely inhibit glycolysis in isolated adult rat myocytes (personal communication). All incubations were carried out in open flasks in a shaking metabolic incubator at 30 C.

Aliquots of cells for analysis of viability and morphology were obtained with glass capillary tubing and were immediately mixed on a microscope slide with an equal volume of 1% glutaraldehyde in modified Tyrodes solution¹³ to which 0.5 percent trypan blue had been added. Counts of at least 300 cells per slide were completed within 15 minutes of initial sampling. Counts were made of the initial cell isolate of each experiment before incubation and from each of the four samples at 5, 15, 20, 30, 45, and 60 minutes of incubation. Ten separate cell isolations were used for these experiments, all of which filled the criteria of 80–90% squaring by 15 minutes.

The second experiment tested the effect of abrupt swelling on control and metabolically inhibited cells. The experimental protocol is outlined in Figure 1. From each of 7 separate isolates, cells were divided into 2 groups. One group was incubated at 30 C for 25 minutes in isotonic, aerated buffer, without inhibitors, and the second in buffer containing 5 mM IAA and 6 mM Amy. The cells from each group were then subdivided into 2 samples, the cells centrifuged out and resuspended in either isotonic or hypotonic (50 percent dilution with deionized water) buffer. Inhibitors were maintained in the resuspension buffers if they were present originally. Aliquots were sampled for cell counts at 3 and 5 minutes after resuspension.

Morphologic Studies

Cell counting was performed using reduced light with an ordinary $\times 10$ objective. Cells were classified as to being rod-shaped (length/width ratio greater than 3:1), square-shaped (length/width ratio less than 3:1 but greater than 1:1) or round-shaped (length/width ratio less than 1:1 or obvious round shape). Cells were further classified as being trypan blue-excluding (viable) or trypan blue-staining (nonviable). For electron microscopy 0.25 ml aliquots of samples were placed in an equal volume of 1% glutaraldehyde in modified Tyrodes solution (320 mOsm) containing 0.1% tannic acid. When the final sample buffer was hypotonic, the fixative was also diluted one-half with deionized water to maintain hypotonicity during initial fixation. Following 5 minutes of fixation, cells were centrifuged into a pellet and fixation was continued for an additional 1–3 hours. The pellet was then removed and postfixed for 1 hour in 1% osmium tetroxide. The pellet fragments were then processed routinely for plastic embedding for light and electron microscopy.

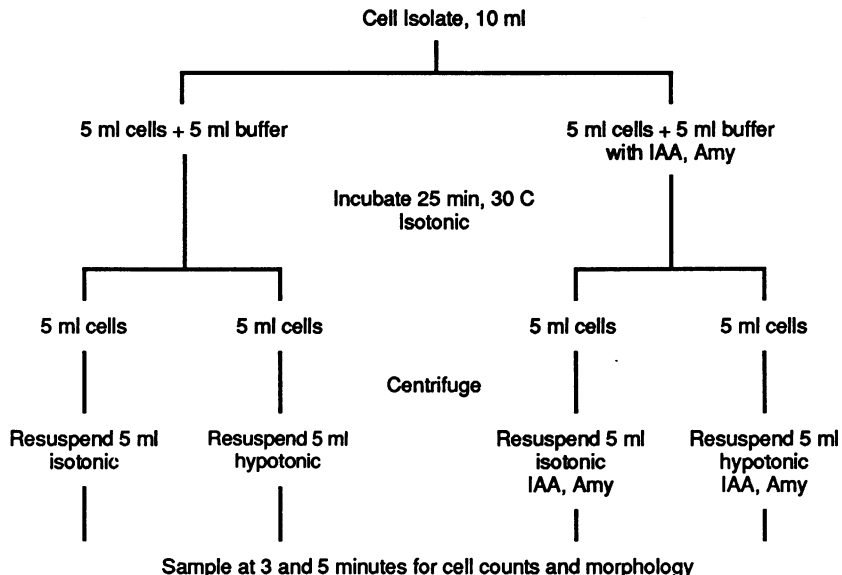
Statistics

Statistical differences between sample means were calculated using a two-tailed paired Student's *t*-test. A *P* value of less than 0.05 was considered significant. The paired test was used because of the natural pairing of the experimental samples, due to the variations in the cell counts of the original isolates for each experiment. A separate isolate was used for each experiment. Values in the text and table are expressed as means and standard deviations. Values in the figures are graphed as means plus or minus the standard error.

Results

Individual cell isolates ranged from 56–80 percent rod-shaped cells with 80–97 percent viability (trypan blue exclusion). Cells at the initiation of the experiment averaged $68.6 \pm 6.0\%$ rods. During isotonic incubations the rods decreased to $61.8 \pm 5.1\%$ (Figure 2). Hypotonic incubation caused an initial decrease in rods to $59.8 \pm 6.9\%$ which decreased further to $53.1 \pm 8.5\%$ by the end of the experiment. In isotonic incubations the percentage of viable round cells was initially $20.8 \pm 5.4\%$. This slowly decreased to $14.7 \pm 5.2\%$ with an inversely parallel increase in nonviable round cells. Hypotonic incubation produced a more rapid decrease in the number of viable round

Figure 1—Flow chart of the experimental design of the experiment to determine the effect of abrupt swelling on previously incubated control and metabolically inhibited cells.



cells. The difference at 5 minutes was $20.9 \pm 7.1\%$ to $16.1 \pm 5.0\%$ for isotonic and hypotonic cells, respectively. This difference was maintained throughout the control incubation period (Figure 2).

Metabolic inhibition of cells with IAA and Amy in isotonic buffer caused a rapid decrease in the population of rod cells (Figure 3). This decrease was mirrored by a similarly rapid increase in the percentage of square cells. After 15 minutes of incubation, the percentage of cells in the incubate was $16.8 \pm 15.7\%$ rods, $39.7 \pm 15.4\%$ viable squares, $17.1 \pm 4.3\%$ viable rounds, $24.9 \pm 4.4\%$ nonviable rounds, and 1.8

$\pm 2.0\%$ nonviable squares. In hypotonic media the corresponding percentages were $18.1 \pm 12\%$ rods, $27.4 \pm 12.6\%$ viable squares, $10.1 \pm 4.6\%$ viable rounds, $33.44 \pm 6.3\%$ nonviable rounds, and $9.7 \pm 10.1\%$ nonviable squares. The rates of squaring of cells in isotonic and hypotonic buffer were similar.

Figure 4 shows the relative percentage of nonviable square cells as compared with the total number of square cells (viable plus nonviable) in the sample during isotonic and hypotonic incubations. There was a more rapid conversion of viable square cells to nonviable square cells during hypotonic, than during isotonic incubations. At 45 minutes of incubation in isotonic buffer there were $13.5 \pm 13.5\%$ nonviable

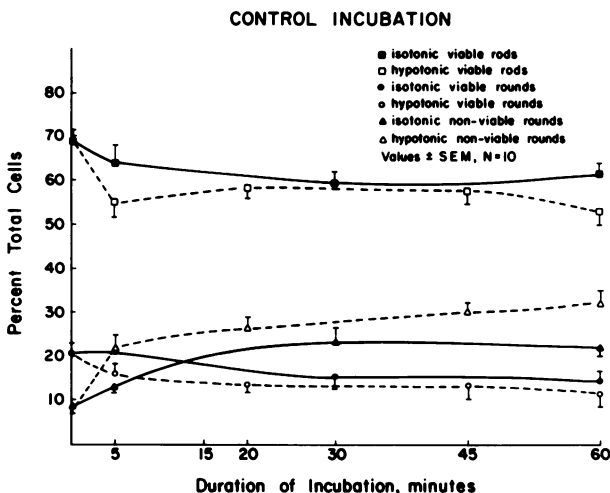


Figure 2—Graph showing the percentage of the various cell types during control incubations in isotonic (closed symbols) or hypotonic (open symbols) buffer. Following an initial small drop in the percentage of rod cells, the preparations remained relatively stable for the duration of the experiment. Viable round cells were converted to nonviable rounds more rapidly during hypotonic than isotonic incubation.

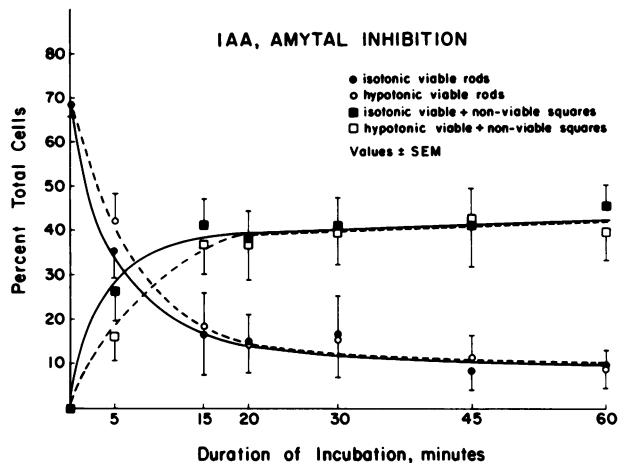


Figure 3—Graph showing the rates of conversion of rod cells to square forms during incubation of metabolically inhibited cells in isotonic (closed symbols) or hypotonic (open symbols) buffer. The rates of conversion were nearly identical in the 2 media.

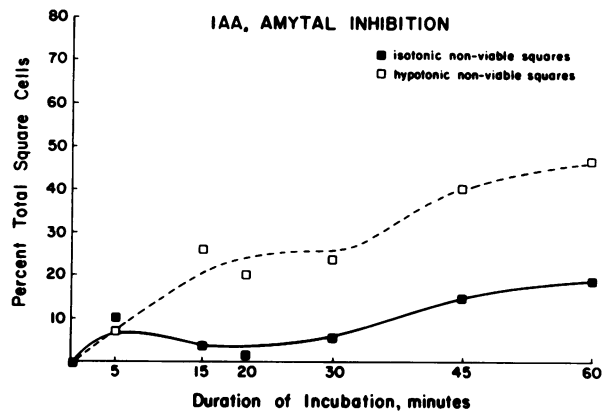


Figure 4—Graph showing the percentage of nonviable square cells [(nonviable squares/viable squares + nonviable squares) × 100] during isotonic (closed symbols) or hypotonic (open symbols) incubation in the presence of metabolic inhibition. The rate of conversion of viable to nonviable square cells was higher in hypotonic buffer than in isotonic buffer.

squares. In hypotonic buffer the percent of nonviable squares was $37.0 \pm 22.0\%$ ($P < 0.01$).

In the second experiment the effects of acute osmotic swelling on control and metabolically inhibited cells were determined. The data shown in Table 1 indicates that control (noninhibited) incubations of cells in either isotonic or hypotonic buffer produced little damage other than a slight decrease in rods and a corresponding increase in viable and nonviable round cells. Metabolic inhibition caused a marked reduction in rods, reflected by an increase in the percent of square cells. Resuspension in hypotonic buffer caused an increased rate of conversion of viable squares to nonviable square cells. At 3 minutes metabolically inhibited cells suspended in isotonic buffer contained $7.8 \pm 4.3\%$ nonviable square cells, while suspension of inhibited cells in hypotonic buffer significantly in-

creased the percentage of nonviable squares to $19.9 \pm 9.6\%$ ($P < 0.005$). Following 5 minutes of swelling, the percent nonviable squares was $14.5 \pm 9.5\%$ and $33.6 \pm 16.1\%$ ($P < 0.001$), respectively, in isotonic and hypotonic buffer.

Cell Morphology

The appearances of isolated myocytes in wet, trypan blue-stained preparations are shown in Figure 5. In control isotonic incubations, most of the cells were rod-shaped and excluded trypan blue. A lesser number of viable and nonviable round cells also were present. The rod cells had well-defined striations and angular or stepped ends (Figure 5A). In control hypotonic incubations, the overall appearance was similar to isotonic preparations. Due to a normally large variation in cell size, morphologic evidence of swelling could only be determined by a somewhat clearer, crystal-like appearance of the rod cells (Figure 5B). In metabolically inhibited isotonic preparations, most of the rod cells had converted to square cells. Most of the square cells excluded trypan blue, but there were also a variable number of blue-staining square cells (Figure 5C). Metabolically inhibited hypotonic incubates also contained a variably large number of blue squares. Examination of these cells under high magnification revealed that an estimated 80% or more possessed clear dome-shaped blebs on their surface and also blebs covering the ends of the intercalated disks. Blebs could also be seen on numerous round cells and on the blue round and square cells in isotonic inhibited preparations. Blebs were rarely seen on either viable rod cells or on viable square cells, however, after hypotonic swelling (Figure 5D).

Table 1—Effects of Hypotonic Swelling on Control and Metabolic Inhibited Isolated Myocytes*

Initial control isolate before incubation (all values: mean ± S.D.)†	Rod	Square	Round	Nonviable round	Nonviable square
	68.7 ± 5.8	1.3 ± 0.9	24.3 ± 5.1	5.9 ± 5.0	—
3 min. control isotonic	60.5 ± 6.0‡	1.2 ± 0.9	19.8 ± 2.7	18.3 ± 4.6‡	—
3 min. control hypotonic	57.8 ± 6.0	1.2 ± 0.7	16.5 ± 3.0	24.4 ± 5.6	—
3 min. IAA, amytal isotonic	3.6 ± 1.8	41.0 ± 5.1	13.9 ± 5.3	33.6 ± 10.3	7.8 ± 4.3
3 min. IAA, amytal hypotonic	2.1 ± 1.6	32.5 ± 5.4§	10.3 ± 3.2	35.3 ± 6.1	19.9 ± 9.6‡
5 min. control isotonic	52.2 ± 4.8	1.2 ± 1.2	17.8 ± 2.4	23.5 ± 5.2	—
5 min. control hypotonic	53.2 ± 7.3	1.4 ± 1.0	14.1 ± 4.1	31.5 ± 7.1	—
5 min. IAA, amytal isotonic	1.9 ± 1.8	36.7 ± 9.6	9.6 ± 5.2	37.2 ± 7.4	14.5 ± 9.5
5 min. IAA, amytal hypotonic	1.0 ± 1.0	20.9 ± 11.3‡	6.1 ± 3.4	38.3 ± 7.0	33.6 ± 16.1‡

* Data from the abrupt swelling experiment. Each value represents the mean and standard deviation of seven experiments. Symbols for statistical significance are indicated for values tested against the preceding value in the same column.

† Twenty-five minute control or IAA, amytal incubation followed by 3-minute or 5 minute incubation in isotonic or hypotonic buffer.

‡ $p < 0.001$.

§ $p < 0.01$.

‡ $p < 0.005$.

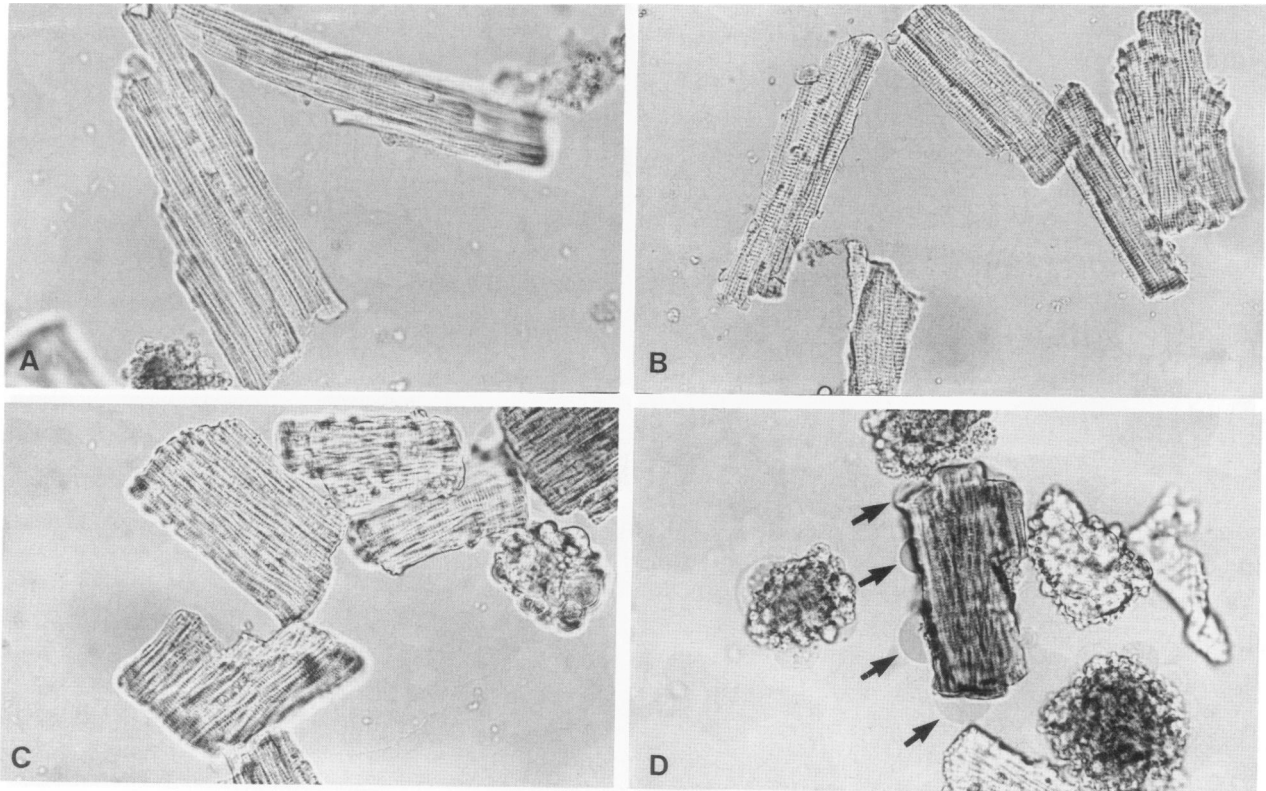


Figure 5—Light micrographs of wet preparations of cells in the presence of trypan blue. **A**—Control isotonic incubation. Most cells were elongated rod shaped forms which excluded trypan blue stain. **B**—Control hypotonic incubation. Most cells retained a relaxed rod shape but had more distinct Z-band striations suggesting some degree of cellular swelling. **C**—Metabolically inhibited isotonic incubation. Portions of five viable square cells are present. The cells are contracted with narrowed Z-band spacings. Blebs were rarely seen on trypan blue-excluding square cells. Also present is a viable round cell and a portion of a nonviable (blue staining) square cell. **D**—Metabolically inhibited hypotonic incubation. Many square cells converted to nonviable, blue-staining forms during hypotonic incubation. There are several dome-shaped blebs on the lateral surface and over the intercalated disk area of this cell (arrows). Also present are three nonviable and one viable round cells, as well as a portion of a viable square cell. All panels $\times 500$

Toluidine blue-stained sections of plastic embedded cells in control isotonic incubated preparations showed a predominant population of uniformly staining rod cells cut in various planes. Spacing of Z-bands was well delineated and intercalated disk ends were angular. Two types of round cells could be distinguished. One stained darkly and had a central, dense, disk-shaped core surrounded by membrane protrusions. The second type of round cell maintained a dense central core but the surrounding cytoplasm was less dense and appeared to have irregular margins. These 2 cell types were believed to correspond to viable and non-viable cells respectively as seen in the wet preparations (Figure 6A). The appearance of rod cells in hypotonic preparations differed only in that the staining of cells tended to be less intense; there was a uniform dispersion of nuclear chromatin and there was often a large perinuclear space (Figure 6B). Metabolically inhibited cells in both the isotonic and hypotonic preparations were similar except that the nuclear chromatin was again dispersed and the cells

stained less intensely in hypotonic preparations (Figures 6C, D).

In both preparations varying proportions of 2 types of contracted square cells were observed. The first type had close sarcomere Z-band spacing and sharp borders. The second was similar except that single or multiple blebs could be seen protruding from the lateral cell surface and covering the ends of the cells. These blebs differed from the cytoplasmic protrusions seen on round cells in that the blebs usually contained few organelles, while the round cell protrusions usually were filled with mitochondrial-sized objects.

Electron microscopy extended the light microscopic findings. Control isotonic rod cells had relaxed sarcomeres and intact sarcolemmal membranes. These cells resembled control cells from intact hearts. Rod cells from hypotonic preparations were similar in appearance except there was a greater space between cellular organelles, the nuclear chromatin was dispersed, and mitochondrial profiles had irregular, focal, empty spaces considered due to cell swelling.

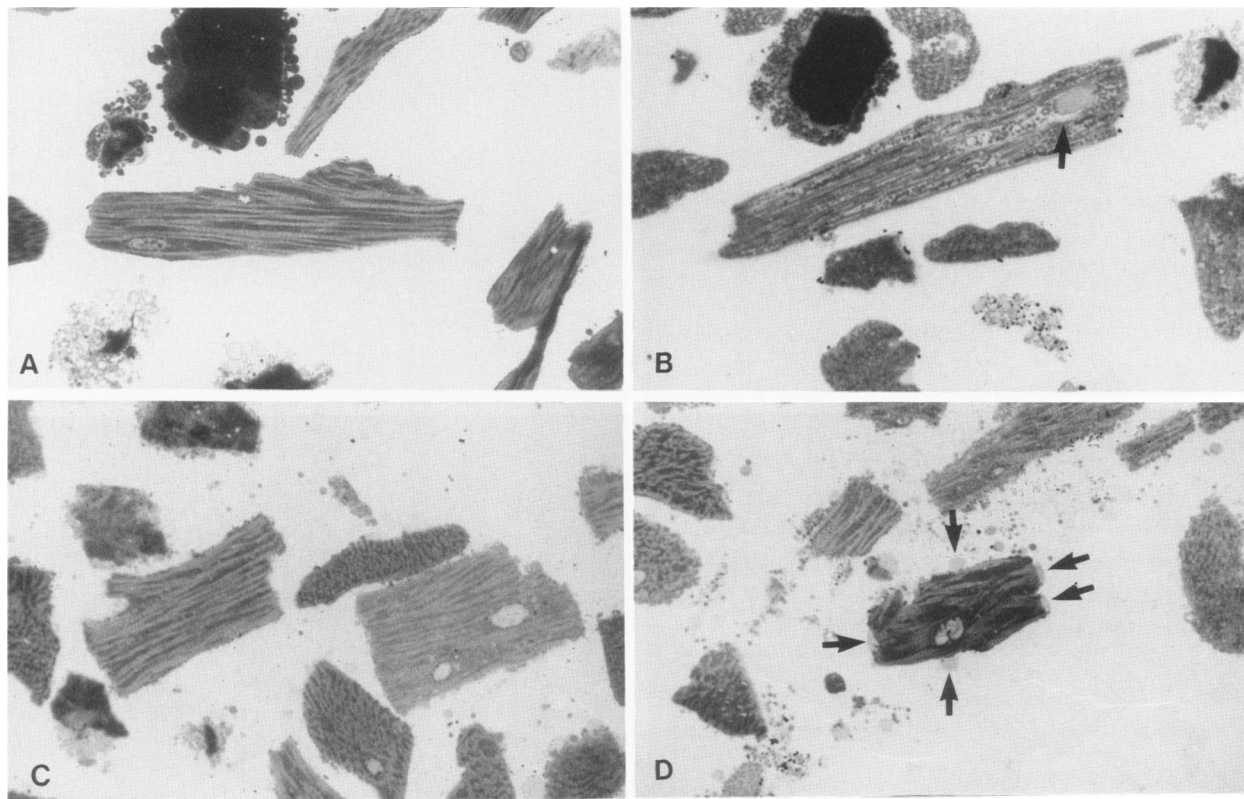


Figure 6—Toluidine blue-stained plastic sections. **A**—Control isotonic incubation. A rod cell and several round cells are present. Other cells are tangentially sectioned rod cells. **B**—Control hypotonic incubation. The rod cells appeared less dense than in isotonic buffer. The dispersed nuclear chromatin and perinuclear space (arrow) are indicative of cell swelling. **C**—Metabolically inhibited isotonic incubation. Most of the cells are contracted into square cells. No subsarcolemmal blebs are seen. **D**—Metabolically inhibited isotonic incubation. Although more frequently present during hypotonic incubations, square cells with lateral blebs and dome-shaped blebs capping the ends of the cells (arrows) were present in both isotonic and hypotonic incubated samples. It is presumed that these cells correspond to the blue squares seen in wet preparations. All panels $\times 500$

In metabolically inhibited preparations most cells were highly contracted, with thickening of Z-bands and absence of I-bands. Many contracted cells, especially in hypotonic preparations, had either lateral blebs or blebs capping the ends of the cells. The lateral subsarcolemmal blebs (Figure 7) covered 1 to several Z-band lengths. The blebs were filled with a loose flocculant material and rarely contained mitochondria. The sarcolemmal membrane covering blebs was usually intact but was occasionally found to contain ruptures. The blebs capping the ends of cells (Figure 8) were formed by a lifting of the sarcolemmal membrane from the terminal ends of the sarcomeres. The dense Z-bandlike material of the intercalated disk fascia adherens junctions remained associated with the sarcomeres. The intervening bleb space was filled with flocculant material and a few mitochondria or other organelles.

Discussion

Isolated, calcium tolerant, adult myocytes are quiescent and maintain an elongated rod shape during

control incubations.¹⁴ These cells exclude trypan blue, retain nearly normal ATP levels,^{15,16} and have an ultrastructural appearance similar to normal cells from *in vivo* heart tissue.¹⁷

Rod cells will hypercontract into round (actually disk-shaped) forms if intracellular calcium levels are raised.^{6,12,14,18} This can be done by increasing the sodium content of cells by transient calcium-free incubation, cold incubation, or ouabain-induced inhibition of the sodium-potassium pump. These round cells, like the rod cells, remain viable with nearly normal ATP levels. Round cells also form during conventional hypoxic incubations using commercial gas mixtures. This type of rounding is thought to be due to a critically low ATP level, which does not allow full relaxation but rather maintains the presence of enough rigor complexes to activate contraction while also supplying enough ATP to support contraction (rigor contracture).¹⁸ In both cases, round cells (unlike rod cells) are relatively fragile, so that mechanical trauma (such as vigorous stirring) converts viable rounds into nonviable, blue-staining rounds.⁷ The

cause of this mechanical fragility is uncertain, but may be related to the large cytoplasmic protrusions that form as the cells distort themselves during hypercontraction.

Square cells are rarely seen in hypoxic experiments¹⁹ unless special precautions are used to ensure ambient oxygen levels below the 3 torr level, which is sufficient to fully saturate mitochondrial cytochromes. These precautions include use of steel tubing, sealed all-glass incubation vessels, and ultra-pure gas.²⁰ Square cells are in a contracted state with nearly zero cytosolic ATP levels, and will remain square if ATP production is totally inhibited. Even very low levels of ATP production will convert the squares to rounds.¹¹ Chemical blockade (used in the present study) is a technically simpler method of achieving nearly total inhibition of aerobic and anaerobic ATP production and therefore a stable population of square cells. Square cells initially exclude trypan blue, but with continued incubation convert into blue-staining, nonviable square cells that remain square for an additional several hours of incubation.

It should be pointed out that in the present experiments perfect metabolic blockage was not obtained in experiments using 3mM Amytal. This was apparently due to a loss of potency of the drug, which requires the dose to be increased to 5 mM during the course of the experiments. This incomplete inhibition of mitochondria probably accounts for the production of small numbers (10–20%) of round cells, as can be deduced by examination of Figure 3. As compared with the results of previous experiments¹¹ where metabolic inhibition was obtained, there was almost no increase in the numbers of round cells during incubation.

In some cell culture systems the use of trypan blue staining to indicate nonviability has been justified. Trypan blue staining has been correlated with the release of cytosolic enzymes from cells into the incubation medium, which is associated with the rupture of the plasma membrane.^{7,21–23} Because cell viability is dependent on an intact plasma membrane, blue-staining cells are justifiably considered to be dead.

In these studies, trypan blue was mixed into the glutaraldehyde fixative to be used for cell counts. Glutaraldehyde can maintain the permeability properties of cell membranes for short periods of time. Preliminary studies confirmed that counts of fixed and unfixed preparations are the same if the fixed cells are counted within 15–20 minutes. After this time, dye slowly leaks into an increasing number of cells, making counts unreliable. On counting slides, the shapes of fixed cells remain stable, whereas unfixed cells degenerate, making accurate cell counts impossible. In this

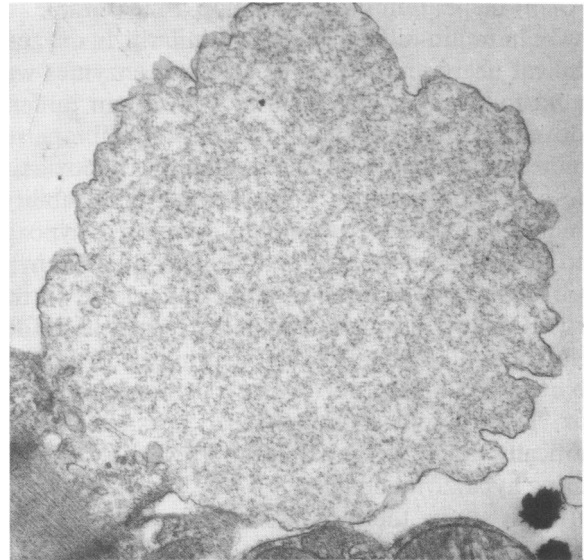


Figure 7—Electron micrograph of a small lateral subsarcolemmal bleb. The protruding sarcolemma has detached from a Z-band. The bleb is filled with flocculant and fibrillar material but contains no mitochondria or other organelles. $\times 14,000$

study, all slides were counted within 15 minutes of the time of sampling.

Responses of Isolated Myocytes to Hypotonic Incubations

Steenbergen, Hill, and Jennings¹ have found that control dog heart slices subjected to hypotonic (60

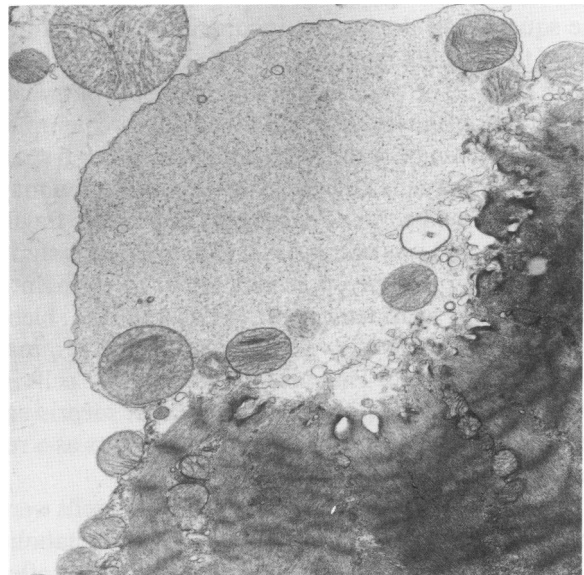


Figure 8—Electron micrograph of an intercalated disk membrane bleb at the end of a square cell. The sarcomeres are contracted. The sarcolemma has separated from the terminal actin filaments of the sarcomere chain. The dense material associated with the fascia adherens junction remains associated with the ends of the actin filaments. $\times 7000$

mOsm) incubation do not develop a measurable increase in inulin-diffusible space. Similarly, in oxygenated rat hearts, no release of cytosolic enzymes was found following perfusion with 150 mOsm buffer.² Both results indicate that the plasma membrane remained intact. In contrast, in both studies hypoxic tissues showed increased sarcolemmal permeability, which was dependent on both the duration of hypoxia and the osmolarity of the extracellular fluid. In hypoxic hearts, the occurrence of enzyme release during 150 mOsm perfusions corresponded closely to the development of irreversible injury, as judged by susceptibility of a parallel group of hearts to the oxygen paradox. These results show that heart cells become osmotically fragile as they become irreversibly injured during hypoxic incubations.²

In this study, the response of isolated cells to osmotic stress depended upon the cell type and the previous incubation conditions: 1) Rod cells showed hypotonic swelling but they excluded trypan blue. 2) Viable round cells (in either oxygenated media or with metabolic inhibition) were converted to nonviable cells by hypotonic incubations. The cause of osmotic fragility of round cells is not established, but it may be related to the cytoplasmic protrusions seen on these cells. Such protrusions may be structurally weak as a result of damage to membrane-supporting structures during cell rounding. 3) The osmotic fragility of square cells depended on the duration of incubation after onset of squaring. Thus squaring itself did not cause osmotic fragility. Rather, events occurring in the square cells during the incubation period subsequent to squaring rendered the cells susceptible to osmotic stress. The observation that over 80% of trypan blue-staining square cells contained subsarcolemmal blebs, while such blebs were rarely seen on trypan blue-excluding cells, suggests that bleb formation may be an event related to development of osmotic fragility. Although it was not possible to prove in this study that blebbing actually preceded entry of stain into cells, it would seem reasonable to postulate that blebs formed as a result of swelling prior to sarcolemmal membrane rupture. That blue-staining square cells in isotonic media also possessed blebs is not surprising, because in isotonic media cell swelling occurs as a result of colloid-osmotic pressure.

In the second set of experiments in which cells were abruptly swollen following 25 minutes of metabolic inhibition, the finding that more cells were blue after 5 minutes than after 3 minutes of acute swelling was unexpected. Osmotic cell swelling occurs rapidly. The rate of osmotic swelling is determined by the reflection coefficient of the plasma membrane to water, rel-

ative to solute.²⁴ Therefore a rapid conversion of viable to nonviable forms was expected. Because the time interval between 3 and 5 minutes is too short to allow significant additional hypoxic injury to occur, this result suggests that factors in addition to swelling may contribute to sarcolemmal membrane rupture. Analogous to the mechanical fragility of round cells discussed above, it is postulated that square cells with subsarcolemmal blebs may show both osmotic and mechanical fragility. Although the cells were gently shaken during incubations, the mechanical trauma of colliding cells or Brownian motion of small particles could contribute to damage of the plasma membrane overlying the blebs.

Relationships Between Osmotic Fragility and Irreversible Injury

Irreversible injury can be defined as the inability of cells to survive after removal of the injuring agent and restoration of cells to a normal environment. It is theoretically possible that irreversibly injured cells would be capable of prolonged survival under special conditions or even capable of repair. Cell death is related to loss of plasma membrane integrity.²⁵ Once the permeability barrier of a cell has been breached, the flooding of the cell with calcium and loss of essential cytosolic components would preclude any possibility of survival. In the present study, irreversible injury is presumed to have occurred at the time that cells developed osmotic fragility. Cell death would then have occurred when the cells that were swollen or otherwise traumatized developed rupture of sarcolemmal membranes and became permeable to trypan blue. It is postulated that the basis for osmotic fragility (and presumably also irreversible injury) rests in events that weaken sarcolemmal membrane attachments to underlying cytoskeletal components of the cell, ie, the lateral Z-band attachment sites at costamere junctions, and the attachments of the sarcomere chain to the internal face of the intercalated disk. This weakening becomes manifest upon swelling and results in formation of subsarcolemmal blebs that are presumed to be inherently fragile.

Steenbergen, Hill, and Jennings³ first described a loss of immunofluorescence staining for the cytoskeletal protein vinculin in ischemic myocardium. The authors have confirmed this finding in hypoxic rat hearts⁴ and in addition have found a similar loss of staining for α -actinin. Vinculin occurs specifically at attachment sites of actin to sarcolemmal membranes, at costamere junctions, and intercalated disks. Alpha-actinin is the major dense component of Z-bands and

intercalated disks, and is thought to link actin filaments. Loss or alteration of either or both of these proteins is a possible mechanism of increased cell fragility and irreversible injury. It has been postulated that activation of calcium-activated neutral proteases (CANP) occurs during hypoxia or ischemia. CANPs can specifically remove α -actinin from isolated myofibrillar fractions²⁶ and are, in addition, general proteases. CANPs are, however, sulphhydryl-dependent enzymes that *in vitro* are readily inhibitable by low concentrations of iodoacetic acid.²⁷ In view of the fact that injury in this study proceeded in the presence of high extracellular concentrations of iodoacetic acid (which were capable of inhibiting glycolysis), the possibility that other classes of proteolytic enzymes or even unrelated mechanisms may initiate irreversible cell injury must be considered.

The possibility exists that isolated myocytes may have sustained some degree of sarcolemmal or cytoskeletal damage during the isolation procedure that predisposes the cells to rapid injury during metabolic inhibition. The absence of interstitial attachments and external supports of isolated myocytes, as compared with cells in intact tissues, also could alter the distribution of stresses to cytoskeletal-sarcolemmal attachment complexes. These factors or some other yet undetermined difference between tissue and isolated myocytes may account for the prominent blebs at intercalated disks in isolated cells that are less evident in cells in intact hearts. Despite these uncertainties the results of this study show that metabolic inhibition, and not simply isolation and incubation of cells, is the cause of increased fragility and subsarcolemmal bleb formation.

The blebs seen in this study probably are similar to those described in anoxic myocyte preparations.²⁸ Similar blebs also occur during anoxic incubation of cultured hepatocytes.²⁹ Both studies suggest that early bleb formation may regress if the cells are reoxygenated prior to the event of bleb rupture. While bleb regression may occur in isolated cells, in intact hearts reoxygenation or reperfusion results in sudden contracture or swelling of cells, events that stress and damage the weakened sarcolemmal membranes. The absence of cell attachments in isolated cell preparations may explain why reoxygenation-associated contracture does not lead to enzyme release (oxygen paradox) in isolated cells as it does in intact hearts.

In conclusion, isolated myocytes develop blebbing and osmotic fragility during prolonged metabolic inhibition. These cells show both the increased osmotic fragility and ultrastructural lesions characteristic of anoxic or ischemic injury in intact, *in vivo* myocar-

dium. The isolated adult myocyte may therefore provide a suitable experimental model for future studies of the pathogenesis of irreversible myocardial injury.

References

1. Steenbergen, Jr. C, Hill ML, Jennings RB: Volume regulation and plasma membrane injury in aerobic, anoxic and ischemic myocardium *in vitro*: Effect of osmotic swelling on plasma membrane integrity. *Circ Res* 1985, 57:864-875
2. Vander Heide RS, Ganote CE: Increased myocyte fragility following anoxic injury. *J Mol Cell Cardiol* 1987, 19:1085-1103
3. Steenbergen CJ, Hill ML, Jennings RB: Cytoskeletal damage during myocardial ischemia: Changes in vinculin immunofluorescence staining during total *in vitro* ischemia in canine heart. *Circ Res* 1987, 60:478-486
4. Ganote CE, Vander Heide RS: Cytoskeletal lesions in anoxic myocardial injury: A conventional and high voltage electron microscopic and immunofluorescence study. *Am J Pathol* 1987, 129:327-344
5. Piper HM, Spahr R, Hüttner JF, Spieckermann PG: The calcium and the oxygen paradox: Non-existent on the cellular level. *Basic Res Cardiol* 1985, 80:159-163
6. Frank JS, Brady AJ, Farnsworth S, Mottino JG: Ultrastructure and function of isolated myocytes after calcium depletion and repletion. *Am J Physiol* 1986, 250: H265-H275
7. Altschuld RA, Hostelter JR, Brierley GP: Response of isolated rat heart cells to hypoxia, reoxygenation and acidosis. *Circ Res* 1981, 49:307-316
8. Ganote CE: Contraction band necrosis and irreversible myocardial injury. *J Mol Cell Cardiol* 1983, 15:67-73
9. Ganote CE, Humphrey SM: Effects of anoxic or oxygenated reperfusion in globally ischemic, isovolumic, perfused rat hearts. *Am J Pathol* 1985, 120:129-145
10. Elz JS, Naylor WG: The effect of BDM on the reperfusion-induced calcium gain after ischemia (abstr). *J Mol Cell Cardiol* 1986 (Suppl I), 18:213
11. Vander Heide, RS, Angelo JP, Altschuld RA, Ganote CE: Energy dependence of contraction band formation in perfused hearts and isolated adult myocytes. *Am J Pathol* 1986, 125:55-68
12. Altschuld RA, Gibb L, Ansel A, Hohl C, Kruger FA, Brierley GP: Calcium tolerance of isolated rat heart cells. *J Mol Cell Cardiol* 1980, 12:1383-1395
13. Maunsbach AB: The influence of different fixatives and fixation methods on the ultrastructure of rat kidney proximal tubular cells. I. Comparison of different perfusion fixation methods and of glutaraldehyde, formaldehyde and osmium tetroxide fixatives. *J Ultrastruct Res* 1966, 15:242-282
14. Hohl C, Ansel A, Altschuld R, Brierley GP: Contracture of isolated rat heart cells on anerobic to aerobic transition. *Am J Physiol* 1982, 242:H1022-H1030
15. Haworth RA, Hunter DR, Berkoff HA: Contracture of isolated adult rat heart cells: Role of Ca^{2+} , ATP and compartmentation. *Circ Res* 1981, 49:1119-1128
16. Geisbuhler T, Altschuld RA, Trewyn RW, Ansel AZ, Lamka K, Brierley GP: Adenine nucleotide metabolism and compartmentalization in isolated adult rat heart cells. *Circ Res* 1984, 54:536-546

17. Mazewt F, Wittenberg BA, Spray DC: Fate of intercellular junctions in isolated adult rat cardiac cells. *Circ Res* 1985, 56:195–204
18. Lambert MR, Johnson JD, Lamka KG, Brierley GP, Altschuld RA: Intracellular free calcium and the hypercontracture of adult rat heart myocytes. *Arch Biochem Biophys* 1986, 245:426–435
19. Piper HM, Schwartz P, Hütter JF, Spieckermann PG: Energy metabolism and enzyme release of cultured adult rat heart muscle cells during anoxia. *J Mol Cell Cardiol* 1984, 16:995–1007
20. Stern MD, Chien AM, Capogrossi C, Pelto DJ, Lakatta EG: Direct observation of the “oxygen paradox” in single rat ventricular myocytes. *Circ Res* 1985, 56:899–903
21. Murphy MP, Hohl C, Brierley GP, Altschuld RA: Release of enzymes from adult rat heart myocytes. *Circ Res* 1982, 51:560–568
22. Altschuld RA, Wenger WC, Lamka KG, Kindig OR, Capen CC, Mizuhira V, Vander Heide RS, Brierley GP: Structural and functional properties of adult rat heart myocytes lysed with digitonin. *J Biol Chem* 1985, 260:14325–14334
23. Wenger WC, Murphy MP, Kindig OR, Capen CC, Brierley GP, Altschuld RA: Mitochondrial enzyme retention by irreversibly damaged rectangular isolated adult rat heart myocytes. *Life Sci* 1985, 37:1697–1704
24. Length, width, and volume changes in osmotically stressed myocytes. *Am J Physiol* 1986, 251:H1373–H1378
25. Jennings RB, Reimer KA, Steenbergen C: Myocardial ischemia revisited: The osmolar load, membrane damage and reperfusion. *J Mol Cell Cardiol* 1986, 18:769–780
26. Reddy MK, Rabinowitz M, Zak R: Stringent requirement for Ca^{2+} in the removal of Z-lines and α -actinin from isolated myofibrils by Ca^{2+} -activated neutral proteinase. *Biochem J* 1983, 209:635–641
27. Pontremoli S, Melloni E: Extralysosomal protein degradation. *Ann Rev Biochem* 1986, 55:455–481
28. Scharz P, Piper HM, Spahr R, Spieckermann PG: Ultrastructure of cultured adult myocardial cells during anoxia and reoxygenation. *Am J Pathol* 1984, 115:349–361
29. Herman B, Nieminen A-L, Gores GJ, Lemasters JJ: Irreversible injury in anoxic hepatocytes precipitated by an abrupt increase in plasma membrane permeability. *Federation American Societies for Experimental Biology J* 1988, 2:146–151